OPEN

Sonolucent Cranial Implants: Cadaveric Study and Clinical Findings Supporting Diagnostic and Therapeutic Transcranioplasty Ultrasound

Micah Belzberg, BA, Netanel Ben Shalom, MD,† Edward Yuhanna, BA, RDMS,‡ Amir Manbachi, PhD,‡§ Aylin Tekes, MD,¶ Judy Huang, MD,† Henry Brem, MD,† and Chad R. Gordon, DO, FACS*†*

Background: Previously, sonographic evaluation of the intracranial contents was limited to intraoperative use following bone flap removal, with placement of the probe directly on the cortical surface or through a transsulcal tubular retractor. Cranioplasty with sonolucent implants may represent a postoperative window into the brain by allowing ultrasound to serve as a novel bedside imaging modality. The potential sonolucency of various commonly used cranial implant types was examined in this study.

Methods: A 3-phase study was comprised of cadaveric evaluation of transcranioplasty ultrasound (TCU) with cranioplasty implants of varying materials, intraoperative TCU during right-sided cranioplasty with clear implant made of poly-methyl-methacrylate (PMMA), and bedside TCU on postoperative day 5 after cranioplasty.

Results: The TCU through clear PMMA, polyether-ether-ketone, and opaque PMMA cranial implants revealed implant sonoluceny, in contrast to autologous bone and porous-polyethylene. Intraoperative ultrasound via the clear PMMA implant in a single patient revealed recognizable ventricular anatomy. Furthermore, postoperative bedside ultrasound in the same patient revealed comparable ventricular anatomy and a small epidural fluid collection corresponding to that visualized on an axial computed tomography scan.

Conclusion: Sonolucent cranial implants, such as those made of clear PMMA, hold great promise for enhanced diagnostic and therapeutic applications previously limited by cranial bone. Furthermore, as functional cranial implants are manufactured with implantable devices housed within clear PMMA, the possibility of utilizing ultrasound for real-time surveillance of intracranial pathology becomes much more feasible.

Key Words: Cranioplasty, implant, poly-methyl-methacrylate, sonolucent, ultrasound

(*J Craniofac Surg* 2019;30: 1456–1461)

Large-sized cranial defects are repaired with either autologous or synthetic materials.[1,2] Until recently, autologous bone has been considered the "gold standard" due to patient preference for their own tissue, availability, and cost.[1–7] However, over the past decade, mounting reports of bone flap sterile resorption and infection have prompted the widespread use and acceptance of customized cranial implants (CCIs).[5,7–10] The CCIs offer additional benefits over bone stored for prolonged time periods, such as sterility and design shape to reliably address coexisting hard and soft-tissue deficiencies, thus correcting and/or preventing postoperative temporal hollowing.[11,12]

In parallel, both noninvasive and invasive transcranial ultrasound have demonstrated numerous therapeutic/diagnostic applications including neuromodulation for movement disorders, magnetic resonance imaging (MRI)-guided lesion ablation, and local drug delivery via blood brain barrier disruption.[13–16] Unfortunately however, these emerging technologies remain limited by the acoustic properties of cranial bone causing ultrasonic wave attenuation, scattering, and absorption.[13–21]

In contrast to adults, neonates have multiple open fontanelles which serve as naturally occurring acoustic windows, hence diagnostic ultrasound is widely employed and often favored.[22–24] Single-stage cranioplasty presents a newfound opportunity for neurosurgeons to create a synthetic acoustic window by replacing normal bone with a cranial implant composed of sonolucent biomaterial, a material providing minimal to no obstruction of ultrasonic waves. A sonolucent cranial implant would thereby permit "transcranioplasty ultrasound" (TCU) for both diagnostic and therapeutic postoperative applications.[25]

Of the over 100 cranioplasty surgeries performed at our institution over the past year, the most common biomaterials inserted included poly-methyl-methacrylate (PMMA), polyether-ether-ketone (PEEK), and porous polyethylene. As of just recently, custom cranial implants can be made with a novel clear appearance using PMMA, thereby allowing full transparency to visible light and wireless Bluetooth signal transmission with respect to wireless

From the *Department of Plastic and Reconstructive Surgery, Johns Hopkins University School of Medicine, Baltimore, MD; †Department of Neurosurgery, Johns Hopkins University School of Medicine, Baltimore, MD; ‡Department of Radiology, Johns Hopkins Hospital, Baltimore, MD; §Department of Biomedical Engineering, Johns Hopkins University, Baltimore, MD; and ¶Division of Pediatric Radiology and Pediatric Neuroradiology, The Russell H. Morgan Department of Radiology and Radiological Science, Johns Hopkins University School of Medicine, Baltimore, MD.

Received December 19, 2018.

Accepted for publication February 9, 2019.

Address correspondence and reprint requests to Chad R. Gordon, DO, FACS, Director, Neuroplastic and Reconstructive Surgery, Associate Professor of Plastic Surgery and Neurosurgery, Johns Hopkins University School of Medicine, JHOC, 8th Floor, 601 N Caroline St, Baltimore, MD 21287; E-mail: cgordon@jhmi.edu

CG is a consultant for Stryker and Longeviti Neuro Solutions. JH and CG are stockholders of Longeviti Neuro Solutions. The remaining authors report no conflicts of interest.

ISSN: 1049-2275

DOI: 10.1097/SCS.0000000000005454

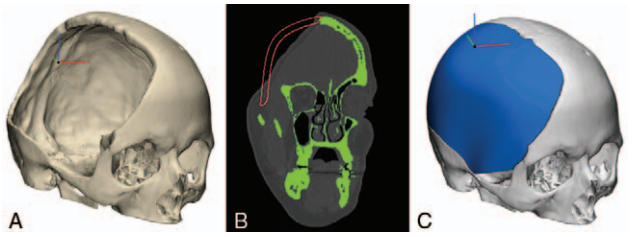

FIGURE 1. Design of patient-specific custom cranial implant made of clear poly-methyl-methacrylate biomaterial. (A) Preoperative 3-dimensional (3D) reconstruction of skull defect from computed tomography (CT). (B) CT of preoperative skull defect in green with patient-specific custom design in red. (C) 3D rendering of customized cranial implant.

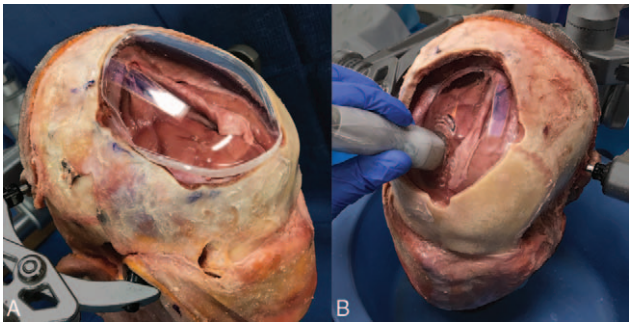

FIGURE 2. Photograph of clear poly-methyl-methacrylate (PMMA) implant and craniectomy defect. (A) Clear PMMA implant during reshaping process. (B) Clear PMMA implant placed within the skull defect, up against the dura. Of note, the scalp has not yet been replaced over the implant. Sonolucency was assessed using a 2.4-MHz transducer with a 3-MHz center frequency. Note that the dura can be seen directly up against the clear cranial implant.

neurotechnology.[26] As such, this served as the impetus for this study, as we hypothesized that clear PMMA implant could also be sonolucent.

MATERIALS

A comprehensive, 3-phase study was utilized in an effort to examine, for the 1st time, the potential sonolucency of all common cranial implant biomaterials versus native bone, and to investigate whether there is potential to incorporate diagnostic/therapeutic ultrasound devices within the actual implant itself as an innovative solution moving forward.[26]

Phase 1: Preclinical Cadaver Study

A preclinical human cadaver study was designed and the specimen obtained via authorized donation from the State of Maryland. We chose to examine synthetic cranial implants composed of porous-polyethylene (Medpor; Stryker, Kalamazoo, MI), PEEK (Kelyniam, Collinsville, CT), opaque PMMA (Stryker), and clear PMMA (Longeviti Neuro Solutions, Hunt Valley, MD). All implants were manufactured to a standard anatomical skull shape and curvature. Implant thickness ranged between 3.0 and 6.5 mm with a mean thickness of 5.4 mm, which is consistent with native bone flap thickness. Ultrasound images were obtained using a 2- to 4-MHz Philips S4-2 sector array broadband transducer and Philips HD 11 XE ultrasound system.

Phase 2: Intraoperative Ultrasound

Following patient's consent, intraoperative ultrasound was performed on a patient undergoing a staged cranioplasty to repair a 15×11 cm right hemicraniectomy defect using a patient-specific 5.2-mm thick implant composed of clear PMMA (Longeviti Neuro Solutions) (Fig. 1). Ultrasound images were obtained using a 1- to 5-MHz Philips S5-1 sector array transducer on a Philips EPIQ 7G ultrasound system.

Phase 3: Postoperative Day 5 Ultrasound

Bedside ultrasound was performed on postoperative day 5 on the patient examined in part 2. Ultrasound images were obtained using a 1 to 5 MHz Philips S5-1 sector array transducer, 3 to 12 MHz Philips L12-3 linear array transducer on a Philips EPIQ 7G ultrasound system.

METHODS

Phase 1: Preclinical Cadaver Study

A human cadaver head was placed in a Mayfield head clamp and an 8 × 7 cm midline-modified bifrontal craniectomy was performed. With the bone flap removed, the expected sunken underlying brain and dura were exposed. All 4 synthetic implants were reshaped in single-stage cranioplasty fashion as described and popularized by the senior author.[25] Hand-held contouring was accomplished using a 5-mm cutting drill based on the dimensions of the excised bone flap. The head was rotated until the craniectomy defect plane was in a horizontal position. Saline was used to fill the cranial cavity and obliterate any epidural dead space. The scalp was then repositioned within the sunken defect against the dura. The scalp was slightly above the water line allowing for application of ultrasound gel. Ultrasound imaging of the scalp covering intact dura and underlying brain was then performed using a sector array transducer with a frequency range of 2 to 4 MHz. The absence of air was assessed using the ultrasound monitor. Images of the ultrasound monitor were then captured as base line control images with no bone or implant present. In step wise fashion, autologous bone, PEEK, porous-polyethylene, opaque PMMA, and clear PMMA implants were each successively placed within the skull defect against the dura (Fig. 2). After positioning of each implant, the native scalp was transposed over the implant, and ultrasound gel was applied. In the clear PMMA trial only, implant transparency also permitted visual inspection of air bubbles beneath the implant. Each implant was imaged using a 2- to 4-MHz sector array transducer and the results are presented within Figure 2. All results were later reviewed by a neuroradiologist to confirm accurate reporting of our findings.

Phase 2: Intraoperative Ultrasound

A 43-year-old man presented for staged cranioplasty repair following decompressive hemicraniectomy. Prior to surgery, a patient-specific cranial implant made of clear PMMA was designed and fabricated (Fig. 1). The implant was modified intraoperatively and inserted per cranioplasty techniques previously described by the senior author.[27] Following implant fixation, and prior to scalp closure, sterile ultrasound gel was applied to the implant surface, the transducer placed within a sterile sleeve, and this was placed on the implant. Intraoperative TCU through the clear PMMA implant was then performed using a 1- to 5-MHz sector array transducer (Fig. 3). Following wound closure, sterile ultrasound gel was again applied to the scalp, the transducer placed on the scalp at the same approximate position, and ultrasound through the clear PMMA implant was performed using a 1- to 5-MHz sector array transducer. A postoperative head computed tomography (CT) was obtained 5 hours postoperatively. Ultrasound and CT results were reviewed with a neuroradiologist to confirm accurate reporting and labeling.

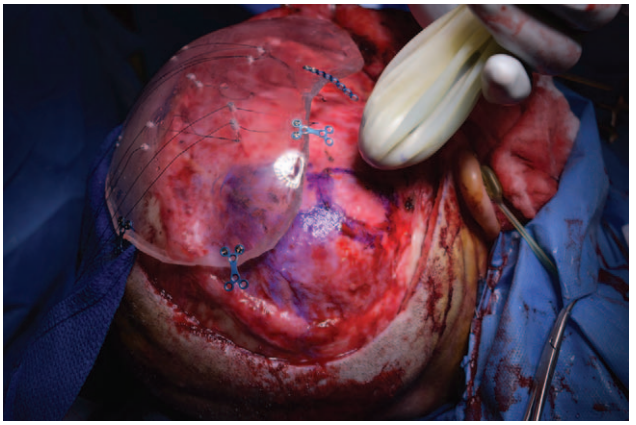

FIGURE 3. Intraoperative photograph of skull defect, clear poly-methyl-methacrylate implant, and ultrasound probe within sterile sleeve.

Phase 3: Postoperative Day 5 Ultrasound

Bedside ultrasound was performed on the same patient in phase 2. The patient's head dressing was removed and sterile ultrasound gel was applied to the scalp. A registered diagnostic medical sonographer then obtained a series of images using both 1 to 5 MHz sector array transducer and 3 to 12 MHz linear array transducers. A head CT was obtained 5 hours later. Ultrasound and CT results were reviewed with a neuroradiologist to confirm accurate reporting and labeling. Of note, patient consent was obtained for inclusion of photographs and all retrospective analyses were conducted via an approved protocol from the Institutional Review Board.

RESULTS

Phase 1: Preclinical Cadaver Study

By way of a standard 2 to 4 MHz sector array transducer, coronal section imaging through "scalp only" (absent bone or implant) displayed different tissue echogenicities during both the static image acquisition and during the sweep through the anatomical area of interest, and bilateral hyperechoic temporal fossa skull bone. Findings suggestive of cadaveric brain tissue could not be visualized with the 2 to 4 MHz ultrasound transducer through the autologous bone flap. Tissue below the bone presented as indistinguishable black images. Similarly, ultrasound using a 2- to 4-MHz sector array transducer could not visualize tissue deep to the implant composed of porous-polyethylene. Ultrasound using a 2- to 4-MHz sector array transducer through PEEK, opaque PMMA, and clear PMMA implants revealed different tissue echogenicities during both the static image acquisition and during the sweep through the anatomical area of interest, and bilateral hyperechoic middle temporal fossa skull bone. Results are presented in Figure 4.

Phase 2: Intraoperative Ultrasound

Intraoperative ultrasound using a sector array transducer with a frequency range of 1 to 5 MHz placed directly on a clear PMMA cranial implant displayed underlying neuroanatomy. Imaging through the implant with the scalp in place slightly reduced the clarity of imaging. Postoperative CT images revealed postoperative changes of epidural air and mixed density epidural collections. Results of phase 2 are presented in Figure 5.

Phase 3: Postoperative Day 5 Ultrasound

Bedside ultrasound through a clear PMMA cranial implant using a 1- to 5-MHz sector array transducer displayed underlying neuroanatomy including brain parenchyma, ventricles with septum pellucidum, temporal lobes, and hyperechoic temporal fossa skull bone. Additionally, ultrasound through a clear PMMA implant using a 3- to 12-MHz linear array transducer revealed a small extradural fluid collection beneath the implant. Review of the corresponding CT images acquired after ultrasound showed absorption of most epidural air seen in the immediate postoperative CT and a small extradural fluid collection beneath the implant. Results of phase 3 are presented in Figure 6.

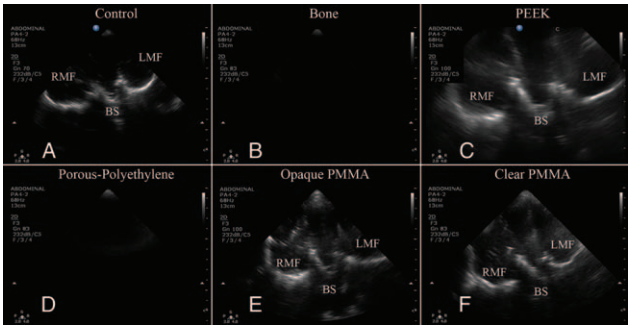

FIGURE 4. Coronal ultrasound imaging of cadaver brain imaged through "scalp only" control, bone, PEEK implant, porous-polyethylene implant, opaque poly-methyl-methacrylate (PMMA) implant, and clear PMMA implant. BS, brainstem; LMF, left middle fossa; RMF, right middle fossa.

DISCUSSION

Ultrasonic waves are significantly distorted and degraded when transmitted through the skull bone thereby limiting the potential for transcranial ultrasound.[28,29] Rising reports of postcranioplasty complications with autologous bone insertion following prolonged freezer or abdominal wall storage have led to increased use of synthetic implants.[5,7–10] For example, a synthetic implant was used in the majority of the over 100 cranioplasty surgeries performed at our institution in the last year. Synthetic implants provide increased sterility and a patient-specific shape to correct both hard and soft-tissue deficiencies.[11,12] As literature reported complication rates following cranioplasty approach 40%, synthetic implants composed of sonolucent biomaterials present a unique opportunity for post-operative complication investigation via diagnostic TCU.[30–32]

A sonolucent implant may permit numerous additional post-operative, ultrasound-based diagnostic, and therapeutic applications including in-clinic assessment of tumor recurrence, cerebral blood flow monitoring, ventricular size measurement for hydrocephalus, midline shift evaluation, nonsurgical modulation for movement disorders, recurrent lesion ablation, and targeted drug delivery through blood brain barrier disruption.[13–19] Furthermore, a sonolucent implant could permit therapeutic ultrasound

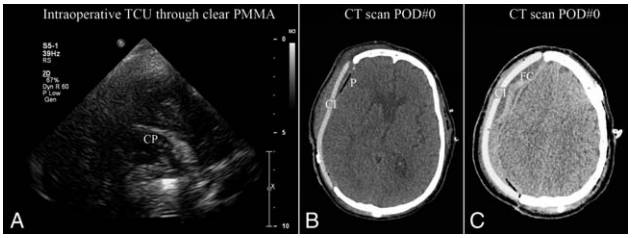

FIGURE 5. Intraoperative transcranioplasty ultrasound (TCU) through clear poly-methyl-methacrylate (PMMA) implant. (A) Ultrasound through scalp and clear PMMA implant showing right choroid plexus (CP) with probe placed on scalp. (B) Postoperative axial computed tomography (CT) showing clear PMMA implant (CI) and pneumocephalus (P). (C) Postoperative axial CT showing clear PMMA implant (CI) and extradural fluid collection (FC).

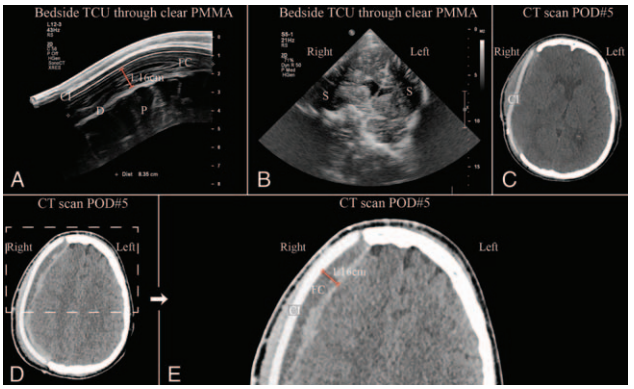

FIGURE 6. Results from postoperative day 5 bedside transcranioplasty ultrasound (TCU) through clear poly-methyl-methacrylate (PMMA) implant. (A) Ultrasound showing clear PMMA implant (CI) with small fluid collection (FC), brain parenchyma (P), and dura (D). (B) Ultrasound showing approximate coronal section with shadow artifacts (S) from titanium clips securing implant. (C) Postop day 5 axial computed tomography (CT) showing clear PMMA implant (CI) and absorption of pneumocephalus. (D) Postoperative axial CT with clear PMMA implant. Dashed region of (D) enlarged in (E). (E) Enlarged region of (D) postoperative axial CT again showing clear PMMA implant (CI) and small extradural fluid collection (FC).

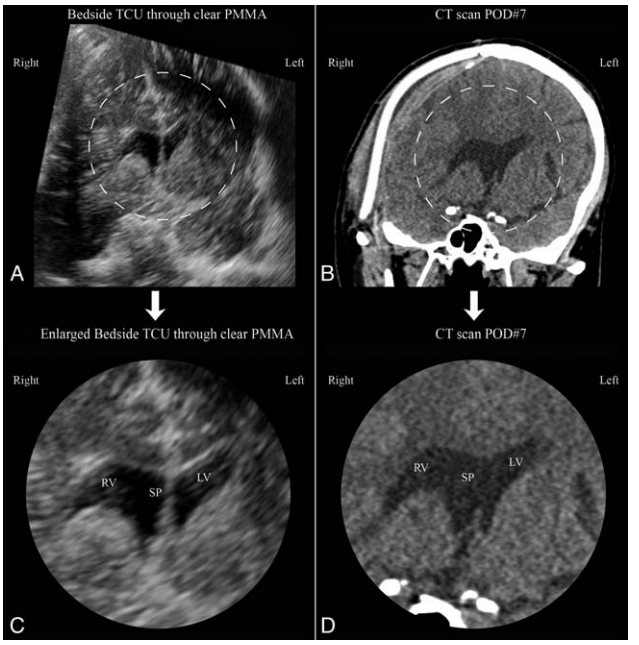

FIGURE 7. Comparison of coronal sections generated with transcranioplasty ultrasound (TCU) through clear poly-methyl-methacrylate (PMMA) implant and computed tomography (CT). (A) Approximate coronal section generated with postoperative day 5 bedside TCU through clear PMMA. Image has been rotated to match standard radiographic image convention. (B) Postoperative day seven CT coronal section at approximate position as ultrasound generated image. Dashed regions of (A) and (B) enlarged and presented as (C) and (D), respectively. (C) Enlarged center portion of (A) postoperative day 5 bedside ultrasound showing right ventricle (RV), septum pellucidum (SP), and left ventricle (LV). (D) Enlarged center portion of (B) postoperative CT (day 7) showing right ventricle (RV), septum pellucidum (SP), and left ventricle (LV).

applications previously reliant on MRI guidance such as TCU-guided ultrasound ablation. In addition, there may be optimal clarity for diagnostic/therapeutic ultrasound devices to be incorporated well within the actual implant itself.[26]

The 3-phase study presented here examined the sonolucency of cranial implants composed of clear PMMA, PEEK, porous-polyethylene, and opaque PMMA via a human cadaver model. In addition, the sonolucency of clear PMMA implant was investigated via both intra- and postoperative TCU imaging in a patient who underwent cranial reconstruction after decompressive hemicraniectomy. These novel findings were observed using noninvasive TCU at bedside by way of widely available ultrasound imaging equipment.

In the preclinical cadaver study, the sonolucency of clear PMMA, PEEK, porous-polyethylene, and opaque PMMA cranial implants were compared to cranial bone. The ''scalp only'' scenario served as a control. As expected, cranial bone was not sonolucent.[21] Similarly, porous-polyethylene was not sonolucent using a 2- to 4-MHz transducer, as no tissue could be visualized. The TCU using a 2- to 4-MHz transducer was successful through implants composed of clear PMMA, PEEK, and opaque PMMA. Imaging through each material displayed different tissue echogenicities both during the static image acquisition and during the sweep through anatomical area of interest. These findings establish for the 1st time that clear PMMA is sonolucent (Fig. 4). Furthermore, this study suggests that PEEK and opaque PMMA are also sonolucent using a 2- to 4-MHz transducer. Given that clear PMMA is transparent and has been shown previously to permit wireless Bluetooth signal transmission using implanted neurotechnology, the observed sonolucency extends the potential advantages of clear PMMA well over the other FDA-approved materials.[26] The results reported here also support Mursch and Behnke-Mursch who found intracranial structures visible through a 4-mm thick PEEK implant using ultrasound at 2.5 and 3.5 MHz.[33] It was the promising results obtained in our phase 1 study that prompted our team to proceed with both intra- and postoperative sonolucency testing of clear PMMA implants.

Intraoperative TCU (via a 1–5 MHz transducer) performed on a patient receiving a clear customized PMMA implant for the repair of a large skull defect allowed identification of neuroanatomical structures including the ventricles and choroid plexus. A 1- to 5-MHz sector array transducer used postoperatively at bedside provided greater image clarity (most likely because epidural air was now absent), demonstrated deep brain parenchyma, ventricles with septum pellucidum, temporal lobes, and hyperechoic temporal fossa skull bone. Additionally, a small epidural collection was revealed using a 3- to 12-MHz transducer. These images were then compared in side-to-side fashion to a CT scan performed as standard protocol, which confirmed the presence of a small extradural fluid collection with mixed attenuation (Fig. 7).

The reduced image clarity observed with intraoperative ultrasound, compared to postoperative day 5 ultrasound, is hypothesized to occur due to extensive extradural air at time of placement (as observed in the immediate postoperative CT). This epidural pneumocephalus was absorbed by day 5, as seen in the corresponding CT scan. These results are both encouraging and suggest perioperative TCU through clear PMMA cranial implants may 1 day be utilized for diagnostic imaging studies either at bedside or in the ambulatory clinic.

Open fontanels in neonates serve as naturally occurring acoustic windows permitting routine use of diagnostic ultrasound. Diagnostic capabilities of ultrasound are dependent on multiple factors including operator proficiency, targeted anatomical area relative to the acoustic window, and the type of pathology being examined. Technologic advances and refined imaging protocols continue to expand and improve diagnostic ultrasound; however, the sensitivity and specificity of ultrasound to evaluate certain pathologies in neonates remains inferior to CT and MRI.[34,35] In the adult neurosurgic patient population, this increased sensitivity may not be of help to the surgical team. A review of CT surveillance scans following elective aneurysm clipping found that neurologically intact patients required 99 head CT scans to obtain 1 head CT

scan that influenced medical management.[36] As TCU diagnostic ultrasound develops and its diagnostic abilities become validated, sonolucent cranial implants may reduce the incidence and cost of postoperative CT scanning by providing a faster, nonionizing, bedside diagnostic radiographic modality.

LIMITATIONS

Phase 1: Preclinical Cadaver Study

The synthetic implants used were of standard curvature with standard thickness consistent to those used in the clinical setting. Though the implants were not printed to match in patient-specific form, each implant was reshaped using a cutting burr in single-stage fashion, as typically performed by the senior author. Ultrasound imaging was limited to the center of the implants to reduce the effects of implant shape along the perimeter.

Air is known to significantly affect ultrasound transmission. The cranial cavity was therefore flooded with saline, implants were submerged beneath the water line and implants were placed directly against the dura. As needed, the implants were adjusted, and absence of air was assured using ultrasound. Though the process was repeated until no air was visible under the implant, some air accumulation may have altered our findings.

Speed of sound, attenuation, and acoustic impedance of polymers like PMMA and PEEK are all variables known to vary slightly with temperature change.[37] However, within our experiments, we assumed all implants were consistent with the ambient room temperature. Although the cadaver and implants were not at normal body temperature, the literature reports only minimal differences within this range.[37]

Imaging was performed using the ''Abdominal'' rather than ''Head'' setting on the ultrasound system. The ''Abdominal'' setting was found to permit better visualization of the ventricles and middle temporal fossa. Image clarity may have been improved with use of the ''Head'' setting.

Assessment of TCU sonolucency was performed by several personnel with clinical experience, but a trained neuroradiologist was not present during image acquisition. Sonolucency was a binary determination confirmed with a neuroradiologist after image acquisition based on either visualization or absence of various tissue densities. Importantly, the precise labeling of each structure in Figures 2 and 3 was performed by a neuroradiologist after image acquisition. Future studies should consider including a neuroradiologist at time of image acquisition and include a detailed evaluation by an experienced neuroradiologist.

Phase 2: Intraoperative Ultrasound

Intraoperative ultrasound was performed by a neurosurgeon manipulating the probe aided by an ultrasound technologist at the console refining ultrasound settings for optimal image capture. As ultrasound is user dependent, the quality of the images obtained were potentially reduced by the fact that the technologist was not the one to physically manipulate the transducer. Though this study was performed on a single patient who received a single implant, the material composition between implants is not expected to vary significantly between implants and therefore the observed sonolucency results should be generalizable for all patients receiving these implant types.

Phase 3: Day 5 Postoperative Ultrasound

Although ultrasound was performed by a technologist with extensive experience imaging neonatal neuroanatomy with transfontanelle ultrasound, a neuroradiologist reviewed and labeled imaging results after image acquisition was complete. Interestingly, imaging with a C9-2 curvilinear array transducer was attempted but the curvature of skull limited contact at the periphery causing shadow artifact at the lateral parts of the image thereby preventing probe use. As this study was performed in a single patient, a clinical series is merited to further explore the role and efficacy of postoperative TCU. Additional studies are also needed to validate diagnostic TCU as well as compare TCU to CT and MRI. Therefore, a clinical series is needed which examines the ability to investigate postoperative complications with TCU and consequently the impact of TCU on patient management.

CONCLUSION

For the 1st time, cranial implants composed of clear PMMA have been shown to appear sonolucent in a cadaver setting, intraoperatively at time of placement, and postoperatively at bedside on day 5. Additionally, PEEK and opaque PMMA implants were also found to be sonolucent in the cadaver setting using a 2- to 4-MHz transducer. These results are encouraging as these sonolucent biomaterials may allow for therapeutic and diagnostic ultrasound applications which have been previously limited by the acoustic properties of cranial bone. Undoubtedly, further investigation of sonolucent implants is warranted and should be expanded to include electromagnetic transmission at a variety of frequencies and wavelengths. Future research will be performed by our team to explore the sonolucent properties of clear PMMA and to determine how these newly discovered advantages may be utilized in establishing a new diagnostic/therapeutic modality of TCU. In addition, we plan to explore how smaller implantable neurotechnology devices could be safely housed within cranial implants to allow for wireless, remote surveillance with future value.[38]

ACKNOWLEDGMENTS

The authors thank Dr Bowen Jiang, Mr Bill Sutton, and the Vista Labs team for their kind assistance with this project.

REFERENCES

1. Piazza M, Grady MS. Cranioplasty. *Neurosurg Clin N Am* 2017;28:257–265
2. Feroze AH, Walmsley GG, Choudhri O, et al. Evolution of cranioplasty techniques in neurosurgery: historical review, pediatric considerations, and current trends. *J Neurosurg* 2015;123:1098–1107
3. Reddy S, Khalifian S, Flores JM, et al. Clinical outcomes in cranioplasty: risk factors and choice of reconstructive material. *Plast Reconstr Surg* 2014;133:864–873
4. Servadei F, Iaccarino C. The therapeutic cranioplasty still needs an ideal material and surgical timing. *World Neurosurg* 2015;83:133–135
5. Gilardino MS, Karunanayake M, Al-Humsi T, et al. A comparison and cost analysis of cranioplasty techniques: autologous bone versus custom computer-generated implants. *J Craniofac Surg* 2015;26:113–117
6. Artico M, Ferrante L, Pastore FS, et al. Bone autografting of the calvaria and craniofacial skeleton: historical background, surgical results in a series of 15 patients, and review of the literature. *Surg Neurol* 2003;60:71–79
7. Pryor LS, Gage E, Langevin C-J, et al. Review of bone substitutes. *Craniomaxillofac Trauma Reconstr* 2009;2:151–160
8. Malcolm JG, Mahmooth Z, Rindler RS, et al. Autologous cranioplasty is associated with increased reoperation rate: a systematic review and meta-analysis. *World Neurosurg* 2018;116:60–68
9. van de Vijfeijken SECM, Munker TJAG, Spijker R, et al. Autologous bone is inferior to alloplastic cranioplasties: safety of autograft and allograft materials for cranioplasties, a systematic review. *World Neurosurg* 2018;117:443–452
10. Wolff A, Santiago GF, Belzberg M, et al. Adult cranioplasty reconstruction with customized cranial implants: preferred technique, timing, and biomaterials. *J Craniofac Surg* 2018;29:887–894

11. Zhong S, Huang GJ, Susarla SM, et al. Quantitative analysis of dual-purpose, patient-specific craniofacial implants for correction of temporal deformity. *Neurosurgery* 2015;11(Suppl 2):220–229
12. Gordon C, Bryndza JR, Bisic T. Patient-specific craniofacial implants. United States Patent #9, 216, 084 B2. Issue December 22, 2015.
13. Hersh DS, Kim AJ, Winkles JA, et al. Emerging applications of therapeutic ultrasound in neuro-oncology: moving beyond tumor ablation. *Neurosurgery* 2016;79:643–654
14. Christian E, Yu C, Apuzzo MLJ. Focused ultrasound: relevant history and prospects for the addition of mechanical energy to the neurosurgical armamentarium. *World Neurosurg* 2014;82:354–365
15. Quadri SA, Waqas M, Khan I, et al. High-intensity focused ultrasound: past, present, and future in neurosurgery. *Neurosurg Focus* 2018;44:E16
16. Weintraub D, Elias WJ. The emerging role of transcranial magnetic resonance imaging-guided focused ultrasound in functional neurosurgery. *Mov Disord* 2017;32:20–27
17. Carpentier A, Canney M, Vignot A, et al. Clinical trial of blood-brain barrier disruption by pulsed ultrasound. *Sci Transl Med* 2016;8:343re2
18. Gutierrez MI, Penilla EH, Leija L, et al. Novel cranial implants of yttria-stabilized zirconia as acoustic windows for ultrasonic brain therapy. *Adv Healthc Mater* 2017;6:
19. Monteith S, Sheehan J, Medel R, et al. Potential intracranial applications of magnetic resonance-guided focused ultrasound surgery. *J Neurosurg* 2013;118:215–221
20. Vignon F, Shi WT, Yin X, et al. The stripe artifact in transcranial ultrasound imaging. *J Ultrasound Med* 2010;29:1779–1786
21. Pinton G, Aubry J-F, Bossy E, et al. Attenuation, scattering, and absorption of ultrasound in the skull bone. *Med Phys* 2012;39:299–307
22. Orman G, Benson JE, Kweldam CF, et al. Neonatal head ultrasonography today: a powerful imaging tool! *J Neuroimaging* 2015;25:31–55
23. van Wezel-Meijler G, Steggerda SJ, Leijser LM. Cranial ultrasonography in neonates: role and limitations. *Semin Perinatol* 2010;34:28–38
24. Salas J, Tekes A, Hwang M, et al. Head ultrasound in neonatal hypoxic-ischemic injury and its mimickers for clinicians: a review of the patterns of injury and the evolution of findings over time. *Neonatology* 2018;114:185–197
25. Berli JU, Thomaier L, Zhong S, et al. Immediate single-stage cranioplasty following calvarial resection for benign and malignant skull neoplasms using customized craniofacial implants. *J Craniofac Surg* 2015;26:1456–1462
26. Gordon CR, Santiago GF, Huang J, et al. First in-human experience with complete integration of neuromodulation device within a customized cranial implant. *Oper Neurosurg (Hagerstown)* 2018;15:39–45
27. Gordon CR, Fisher M, Liauw J, et al. Multidisciplinary approach for improved outcomes in secondary cranial reconstruction: introducing the pericranial-onlay cranioplasty technique. *Neurosurgery* 2014;10:179–180
28. Fry FJ, Barger JE. Acoustical properties of the human skull. *J Acoust Soc Am* 1978;63:1576–1590
29. Aubry JF, Tanter M. MR-guided transcranial focused ultrasound. In: Escoffre JM, Bouakaz A (eds) Therapeutic Ultrasound. Advances in Experimental Medicine and Biology, Vol 880. Springer, Cham, Switzerland, 2016.
30. Janus JR, Peck BW, Tombers NM, et al. Complications after oncologic scalp reconstruction: a 139-patient series and treatment algorithm. *Laryngoscope* 2015;125:582–588
31. Broughton E, Pobereskin L, Whitfield PC. Seven years of cranioplasty in a regional neurosurgical centre. *Br J Neurosurg* 2014;28:34–39
32. Wachter D, Reineke K, Behm T, et al. Cranioplasty after decompressive hemicraniectomy: underestimated surgery-associated complications? *Clin Neurol Neurosurg* 2013;115:1293–1297
33. Mursch K, Behnke-Mursch J. Polyether ether ketone cranioplasties are permeable to diagnostic ultrasound. *World Neurosurg* 2018;117:142–143
34. Blankenberg FG, Loh NN, Bracci P, et al. Sonography, CT, and MR imaging: a prospective comparison of neonates with suspected intracranial ischemia and hemorrhage. *Am J Neuroradiol* 2000;21:213–218
35. Bano S, Chaudhary V, Garga UC. Neonatal hypoxic-ischemic encephalopathy: a radiological review. *J Pediatr Neurosci* 2017;12:1–6
36. Zygourakis CC, Winkler E, Pitts L, et al. Clinical utility and cost analysis of routine postoperative head CT in elective aneurysm clippings. *J Neurosurg* 2017;126:558–563
37. Carlson JE, van Deventer J, Scolan A, Carlander C. "Frequency and temperature dependence of acoustic properties of polymers used in pulse-echo systems," IEEE Symposium on Ultrasonics, 2003, Honolulu, HI, Vol 1, 2003, 885–888.
38. Gordon CR. Low-profile Intercranial Device (LID). US Patent Application Publication #US2018/0338835 A1. Published November 29, 2018.

